JOURNAL of the MEXICAN CHEMICAL SOCIETY

https://www.jmcs.org.mx/

Article

Open Access

J. Mex. Chem. Soc. **2026**, *70(1):e2548*

Received September 5th, 2025
Accepted February 9th, 2026

http://dx.doi.org/10.29356/jmcs.v70i1.2548
e-location ID: 2548

Keywords:
Surface-active ionic liquids, critical micellar concentration, thermodynamic properties, ionic-additives, diffusion

Palabras clave:
Líquidos iónicos surfactantes de cadena corta, concentración micelar crítica, propiedades termodinámicas, aditivos iónicos, difusión

***Corresponding author:**
Rodrigo Mayén-Mondragón
email: rmayen@unam.mx

ISSN-e 2594-0317

Impact of Common Additives on the Micellization Properties of a Short-Alkyl-Chain Surface-Active Ionic Liquid in Aqueous Solution

Elda Elizabeth Villalobos Neri[1], Ulises Páramo García[2], Nohra Violeta Gallardo Rivas[2], Margarita Navarrete Montesinos[3], Rodrigo Mayén-Mondragón[1*]

[1]Unidad de Investigación y Tecnología Aplicadas, Facultad de Química, Universidad Nacional Autónoma de México. Vía de la Innovación 410, Autopista MTY-Aeropuerto Km. 10, Parque PIIT, 66629, Apodaca, Nuevo León, México.
[2]Tecnológico Nacional de México/I. T. Cd. Madero, Centro de Investigación en Petroquímica. Prol. Bahía de Aldhair y Av. de las Bahías, Parque de la Pequeña y Mediana Industria, 89600, Altamira, Tamaulipas, México.
[3]Unidad de Investigación y Tecnología Aplicadas, Instituto de Ingeniería, Universidad Nacional Autónoma de México. Vía de la Innovación 410, Autopista MTY-Aeropuerto Km. 10, Parque PIIT, 66629, Apodaca, Nuevo León, México.

Abstract. The present study explores the influence of common organic and inorganic additives on the micellization behavior of the short-alkyl-chain surface-active ionic liquid 1-methyl-3-hexylimidazolium p-toluenesulfonate ([C$_6$mim][PTS]) in aqueous solution. Although [C$_6$mim][PTS] has shown promise for the dehydration of water-in-oil emulsions, its physicochemical properties remain underexplored. Critical micellar concentration (CMC), surface tension, diffusion coefficients, and thermodynamic parameters were evaluated using UV-Vis spectroscopy, ionic conductivity, and cyclic voltammetry, the latter proving equally reliable for CMC determination. All tested additives reduced both the CMC and surface tension, with amphiphilic organic compounds such as hexadecyltrimethylammonium bromide (CTAB) and sodium dodecyl sulfate (SDS) exhibiting the most pronounced effects. Thermodynamic

J. Mex. Chem. Soc. **2026**, *70(1):e2548*
Regular Issue

ISSN-e 2594-0317

analysis confirmed that micellization is spontaneous, exothermic, and entropically favored across the studied temperature range (300.15–318.15 K). Inorganic salts enhanced micellization primarily through enthalpic contributions, while organic additivespromoted entropy-driven aggregation. Diffusion measurements yielded a reference value on the order of 10^{-5} cm²/s for [C_6mim][PTS] in aqueous solution. These findings highlight the tunable aggregation behavior of [C_6mim][PTS] and support its potential for use in emulsion treatment and environmentally friendly separation processes.

Resumen. El presente trabajo explora la influencia de aditivos orgánicos e inorgánicos comunes en el comportamiento de micelización del líquido iónico surfactante de cadena corta 1-metil-3-hexilimidazolio p-toluensulfonato [C_6mim][PTS]) en solución acuosa. Aunque el [C_6mim][PTS] ha demostrado potencial para la deshidratación de emulsiones agua-en-aceite, sus propiedades fisicoquímicas han sido poco exploradas. Se evaluaron la concentración micelar crítica (CMC), la tensión superficial, los coeficientes de difusión y los parámetros termodinámicos mediante espectroscopía UV-Vis, conductividad iónica y voltametría cíclica, siendo esta última igualmente confiable para la determinación de la CMC. Todos los aditivos probados redujeron tanto la CMC como la tensión superficial, destacando los aditivos orgánicos como el bromuro de hexadeciltrimetilamonio (CTAB) y el dodecil sulfato de sodio (SDS) que resultaron en efectos más pronunciados. El análisis termodinámico confirmó que la micelización del líquido iónico es espontánea, exotérmica y entrópicamente favorecida en el intervalo de temperatura estudiado (300.15 - 318.15 K). Las sales inorgánicas favorecieron la micelización principalmente mediante contribuciones entálpicas, mientras que los aditivos orgánicos promovieron la agregación impulsada por cambios en la entropía. Las mediciones de coeficiente de difusión arrojaron un valor de referencia del orden de 10^{-5} cm^2/s para el [C_6mim][PTS] en solución acuosa. Estos hallazgos destacan el comportamiento de agregación modulable de [C_6mim][PTS] y respaldan su potencial para aplicaciones en el tratamiento de emulsiones y procesos de separación ambientalmente sostenibles.

Introduction

Imidazolium-based ionic liquids have garnered significant attention due to their highly tunable physicochemical properties, which make them attractive candidates for a wide range of applications. Achieving a low volatility [1], low flammability [2], high ionic conductivity [3], and remarkable thermal and electrochemical stability [2,4] enable their use in electrochemical devices and analytical applications, advanced materials development and environmental protection [5]. Additionally, their role in extraction, separation, and catalytic organic reactions highlights their versatility for industrial applications [5].

Imidazolium-based ionic liquids having long aliphatic chains, typically exceeding eight carbon atoms, fall into the category of surface-active ionic liquids (SAILs) [6]. SAILs molecular structures confer strong surfactant properties, enabling them to facilitate organic reactions in aqueous media with improved efficiency [6]. At low concentrations, SAILs can enhance reaction outcomes while reducing production costs, which is particularly relevant given that ionic liquids are typically expensive additives. [6]. A fundamental parameter for SAILs in aqueous systems is the critical micellar concentration (CMC). Accurate determination of the CMC is essential for optimizing surfactant efficiency, understanding solvation effects, designing specific aggregation behaviors, and preventing excessive use. Furthermore, by minimizing the required concentration of ionic liquids, manufacturers can more easily comply with safety regulations for wastewater disposal, preventing excessive ionic liquid contamination in aquatic ecosystems. In this direction, recent studies have investigated how organic and inorganic additives interact with ionic liquids in water, uncovering synergistic effects [7-9] that can improve pollutant extraction efficiency at reduced ionic liquid concentrations. Given their diverse roles in such a broad range of applications, the precise characterization of the micellization properties of ionic liquids is crucial to improving performance, reducing environmental impact and broadening industrial implementations.

Ionic-liquids not exhibiting strong acidity or basicity are sometimes called Neutral Ionic Liquids (NIL) [10]. These compounds are suitable candidates for green chemistry applications [11,12]. Notably,

http://dx.doi.org/10.29356/jmcs.v70i1.2548

J. Mex. Chem. Soc. **2026**, *70(1):e2548*
Regular Issue

ISSN-e 2594-0317

Imidazolium-based NILs have been employed in the synthesis of organic compounds for the food and cosmetic industry [13], in microwave-assisted synthesis and dehydration processes [12,14] and in polymerization processes [15]. Their ability to support such transformations while offering environmental and economic benefits reinforces their importance in sustainable practices.

The present study focuses on the micellization behavior of 1-methyl-3-hexylimidazolium p-toluenesulfonate ([C_6mim][PTS]), a short-alkyl-chain surface-active ionic liquid of neutral character. Short-alkyl-chain ionic liquids can exhibit larger diffusion coefficients, higher ionic conductivities, and lower aquatic toxicity compared to their longer-chain counterparts [16,17]. Moreover, interactions with organic and inorganic additives may facilitate micellization at lower CMC values, potentially mimicking advantageous behaviors observed in longer-chain ionic liquids [9,18]. Despite such promising characteristics, [C_6mim][PTS] remains largely unexplored beyond previous publications from our research group [16,19,20]. Expanding investigations into its micellization properties could unlock new applications, particularly in environmental remediation efforts for oil-polluted water bodies [21-23]. Accordingly, this work examines the influence of several common organic and inorganic additives on the micellization of [C_6mim][PTS], discussing observed variations in CMC, surface tension, and fundamental thermodynamic quantities such as the micellization-Gibbs-energy, enthalpy and entropy.

Materials and methods

Materials

The 1-methyl-3-hexylimidazolium p-toluenesulfonate, [C_6mim][PTS] (molecular weight 338.42 g/mol) ionic-liquid was prepared by means of an anion exchange reaction between 1-methyl-3-hexylimidazole bromide and the sodium p-toluenesulfonate salt. The reaction was carried out in aqueous solution during 24 hours at a temperature of 60 °C under constant agitation. More synthesis details can be found in [19]. Fig. 1 shows the ionic liquid chemical structure.

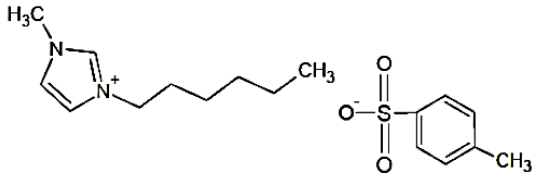

Fig. 1. Chemical structure of 1-methyl-3-hexylimidazolium p-toluenesulfonate ([C_6mim][PTS])

Potassium bromide (KBr), potassium chloride (KCl), sodium sulfate (Na_2SO_4) and ammonium sulfate ($(NH_4)_2SO_4$), all of them purchased from PQM Fermont (analytical grade), were used as inorganic additives. Hexadecyltrimethylammonium bromide (CTAB), Tetramethylammonium chloride (TMAC), Sodium dodecyl sulfate (SDS) and Sodium p-toluenesulfonate (SPTS), all of them purchased from Sigma Aldrich (analytical grade), were used as organic additives. Deionized water ($2x10^{-6}$ S cm^{-1}) was used to prepare all aqueous solutions.

Critical micellar concentration (CMC) of the ionic-liquid in aqueous-solution containing additives

Ultraviolet-visible absorption spectroscopy (UV-Vis) measurements, ionic conductivity determinations and cyclic voltammetry measurements were performed at 301 K (laboratory-temperature). For each tested additive, the ionic-liquid concentration in the aqueous solutions was varied from 0.029 to 0.354 mmol/L. The concentration of inorganic additives was 0.420 mmol/L (50 mg/L) for KBr, 0.670 mmol/L (50 mg/L) for KCl, 0.352 mmol/L (50 mg/L) for Na_2SO_4 and 0.378 mmol/L (50 mg/L) for $(NH_4)_2SO_4$. The concentration of organic additives was 0.109 mmol/L (40 mg/L) for CTAB, 0.456 mmol/L (50 mg/L) for TMAC, 0.138 mmol/L (40 mg/L) for SDS and 0.308 mmol/L (60 mg/L) for SPTS.

http://dx.doi.org/10.29356/jmcs.v70i1.2548

J. Mex. Chem. Soc. **2026**, *70(1):e2548*
Regular Issue

ISSN-e 2594-0317

UV-Vis spectra were acquired with an Agilent Cary 60 spectrophotometer, in the wavelength range from 200 to 800 nm. The absorbance peak in the 200 to 250 nm range was selected to determine the ionic-liquid CMC value. The latter is the concentration of ionic liquid at which the slope of the peak-absorbance versus concentration curve changes [24]. Ionic conductivities were measured using an Orion Star™ A122 Thermo Scientific™ conductivity meter. Each value was recorded once a stable reading was attained (the stabilization time varied with ionic liquid concentration, generally increasing as concentration increased. The maximum waiting period was 30 seconds). CMC values were determined from the specific-conductivity versus ionic-liquid-concentration curves [25]. Cyclic voltammetry was conducted using a BASi 100 B/W potentiostat, a conventional glass cell (25 ml) and the typical 3-electrode configuration. A silver wire (Craft Wire, 925) served as reference electrode, a 304 stainless-steel plate (geometric area 4.6 cm^2, Palmexico Steels) was used as counter electrode and a 304 stainless-steel perforated-plate (geometric area 3.7 cm^2, Palmexico Steels) served as working electrode. Cyclic voltammograms were recorded scanning the potential from -1.8 V to +1.2 V at 0.5 V/s. The anodic peak-values were plotted versus the ionic-liquid concentration to determine the CMC [19]. All measurements were performed in triplicate and the average value is reported. The error bars represent one standard deviation of uncertainty.

The degree of CMC-reduction attained by the additive (η_{CMC}) was calculated as follows:

$$\eta_{CMC} = \frac{CMC_0 - CMC}{C_{ADD}} \qquad \text{Eq. 1}$$

where *CMC* is the critical-micellar-concentration of the ionic-liquid in the solution containing additives, CMC_0 is the critical-micellar-concentration of the ionic-liquid in the solution without additives (0.449 mmol/L [19]) and C_{ADD} is the additive concentration. Equation 1 describes how effectively an additive lowers the CMC per unit of its own concentration. A higher η_{CMC} value indicates a more efficient stabilizing effect by the additive. This metric allows for direct comparison between additives, even if used at different concentrations, by normalizing their effect on micellization.

Surface tension of the ionic-liquid aqueous-solution with/without additives

The surface tension of the aqueous solutions was determined by the sessile-drop method using an Attension One tensiometer (Biolin Scientific) [26]. A ground-glass plate (25x76 mm, thickness 1.2 mm, Pearl) was used as solid surface. All measurements were performed at 301 K (laboratory-temperature). The measurements were repeated until the experimental values were found reproducible. The additives concentration is as previously indicated (CMC determinations). The ionic liquid, however, was added at a concentration equal to its CMC in each solution.

The effectiveness of the surface tension reduction (Π_{CMC}) attained by the ionic-liquid/additive mixture was calculated as shown in Eq. 2a [27]:

$$\Pi_{CMC} = \gamma_0 - \gamma_{CMC/ADD} \qquad \text{Eq. 2a}$$

where γ_0 is the surface tension of bidistilled water (72.1 mN/m) and $\gamma_{CMC/ADD}$ is the surface tension of the ionic-liquid/additive solutions.

The additive effectiveness to decrease the surface-tension of the ionic liquid aqueous solution (η_γ) was evaluated by means of Equation 2b:

$$\eta_\gamma = \frac{\gamma_{CMC} - \gamma_{CMC/ADD}}{C_{ADD}} \qquad \text{Eq. 2b}$$

where γ_{CMC} is the surface tension of the ionic-liquid solution without additive. Equation 2b compares the surface tension of the ionic liquid solution to that of the solution with ionic liquid and additive, normalized by the additive concentration. It measures how effective per unit concentration the additive is in lowering surface tension beyond what the ionic liquid by itself achieves.

http://dx.doi.org/10.29356/jmcs.v70i1.2548

J. Mex. Chem. Soc. **2026**, *70(1):e2548*
Regular Issue

ISSN-e 2594-0317

Diffusion coefficient (*D*) of the ionic-liquid in aqueous solution containing additives

The concentration of additives and ionic liquid in the aqueous solutions is as previously indicated (surface tension measurements). Cyclic voltammograms were acquired with the BASi 100 B/W potentiostat and the glass-cell/3-electrode configuration previously described. The potential was scanned from -1.8 V to +1.2 V at scan rates from 10 to 120 mV/s. The ionic-liquid diffusion-coefficient was determined from the anodic peak-current using the following equation (Eq. 3) for electrochemically irreversible systems [28]:

$$I_{pa} = 0.4958FSC_oD^{1/2}v^{1/2}(\frac{\alpha F}{RT})^{1/2} \quad \text{Eq. 3}$$

where I_{pa} is the anodic peak-current (A), F is the Faraday constant, S is the estimated microscopic electrode area ($1.09\text{x}10^{-3}$ m^2), C_O is the ionic liquid concentration (mol/m^3), v is the potential scan rate (V/s), R is the universal gas constant (J/mol K), T is the absolute temperature (K), D is the diffusion coefficient (m^2/s) and α is the electrochemical reaction charge-transfer-coefficient (~ 0.5). Equation 3 considers n =1 electrons transferred in the anodic reaction. D was determined from the slope (m) of the I_{pa} vs $v^{1/2}$ plot as indicated next (Eq. 4):

$$D = \left(\frac{m}{0.4958FSC_o(\frac{\alpha F}{RT})^{1/2}}\right)^2 \quad \text{Eq. 4}$$

Thermodynamic analysis of micellization

The critical-micellar-concentration and β parameter (degree of counterion binding, i.e. fraction of counterions bound to the surfactant ion [29]) temperature-dependence was studied by means of ionic conductivity measurements. Aqueous solutions were prepared with the ionic-liquid concentration varying from 0.029 to 0.472 mmol/L. The additives concentration is as indicated in previous sections. The analysis was performed at five different temperatures from 300.15 to 318.15 K using an Orion Star™ A122 Thermo Scientific™ conductivity meter. The solution temperature was controlled by means of a circulating-water bath (BHS-1, JOANLAB). Ionic conductivities were recorded only after a stable reading was attained. The β parameter was calculated from the slope of the pre- and post-CMC regions on the specific-conductivity versus ionic-liquid-concentration curve [29,30]. The corresponding plots can be found in the supplementary information. The CMC and β values were used to determine the Gibbs energy (ΔG_m), enthalpy (ΔH_m) and entropy (ΔS_m) of micellization [29-31]. According to the mass-action model of micellization, ΔG_m is related to the CMC and β parameter as indicated in Equation 5 [29,30]:

$$\Delta G_m = (1+\beta)RTlnX_{CMC} = (1+\beta)RTln\frac{CMC}{55.4} \quad \text{Eq. 5}$$

where X_{CMC} is the CMC mole-fraction calculated by dividing the CMC (mol/L) by 55.4 mol/L (molar density of water at 301K). ΔH_m was determined by means of the Gibbs-Helmholtz equation (Eq. 6) [30]:

$$\Delta H_m = \left[\frac{\partial\left(\frac{\Delta G_m}{T}\right)}{\partial\left(\frac{1}{T}\right)}\right] = -T^2\frac{\partial\left(\frac{\Delta G_m}{T}\right)}{\partial T} = -(1+\beta)RT^2\left[\frac{\partial ln\left(\frac{CMC}{55.4}\right)}{\partial T}\right] \quad \text{Eq. 6}$$

Finally, ΔS_m was calculated from ΔG_m and ΔH_m as indicated in equation 7 [31]:

$$\Delta S_m = \frac{\Delta H_m - \Delta G_m}{T} \quad \text{Eq. 7}$$

http://dx.doi.org/10.29356/jmcs.v70i1.2548

J. Mex. Chem. Soc. **2026**, *70(1):e2548*
Regular Issue

ISSN-e 2594-0317

Results and discussion

Critical micellar concentration of the ionic-liquid in aqueous-solution containing additives

Fig. 2 presents the UV-Vis absorbance spectra (200–250 nm) for the [C_6mim][PTS] solution containing potassium bromide, exhibiting the characteristic behavior of imidazolium-ion aggregates [24]. An absorbance peak appears near 220 nm, with absorption increasing as the ionic liquid concentration rises.

Fig. 3 illustrates the dependence of the peak-absorbance on ionic liquid concentration in the solution containing sodium p-toluenesulfonate. The critical micellar concentration (CMC) is clearly identified by the distinct change in the plot's slope. Beyond the CMC, a lower slope is observed compared to the pre-micellar region, a trend consistent across all tested solutions (Fig. S1, Supplementary Information). The decrease in UV-Vis absorbance following micellization may be due to chromophoric groups becoming encapsulated within the hydrophobic micellar core, thus reducing their interaction with the solvent and altering electronic transitions. [32,33]

Regarding the ionic conductivity measurements, as Fig. 3 shows, the CMC of the [C_6mim][PTS] solution containing sodium p-toluenesulfonate can be identified as well by the distinct change in plot slope. In the pre-micellar region, conductivity increases proportionally with ionic liquid concentration due to the rising number of free ions in solution. However, beyond the CMC, aggregation into micelles, counterion condensation and interactions among micelles and additive ions reduce the solution's current-carrying capacity, leading to a decreased conductivity slope. This trend holds across all tested solutions (Fig. S2, Supplementary Information).

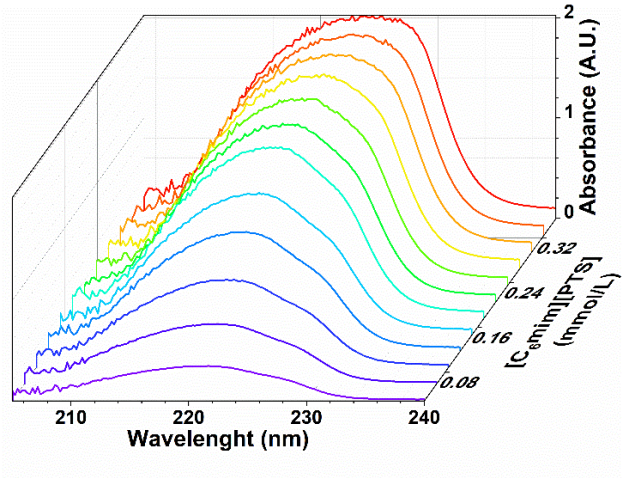

Fig. 2. Absorption spectra of the 1-methyl-3-hexylimidazolium p-toluenesulfonate ([C_6mim][PTS]) aqueous solutions contaning KBr as additive (0.420 mmol/L).

For solutions with inorganic additives, the specific-ionic-conductivity magnitude follows the order: $(NH_4)_2SO_4$ > Na_2SO_4 > KCl > KBr, consistent with the relative ionic strength of the solutions. However, among organic additives, only the TMAC solution aligns with the expected behavior (highest ionic strength), suggesting a complex interplay between organic additive ions and ionic liquid molecules in determining conductivity.

http://dx.doi.org/10.29356/jmcs.v70i1.2548

J. Mex. Chem. Soc. **2026**, *70(1):e2548*
Regular Issue

ISSN-e 2594-0317

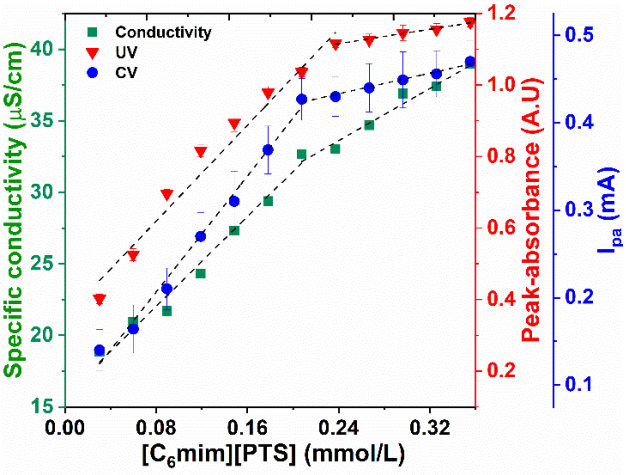

Fig. 3. Peak absorbance, specific conductivity and anodic peak-current (I_{pa}) versus 1-methyl-3-hexylimidazolium p-toluenesulfonate ([C_6mim][PTS]) concentration in aqueous solution containing Sodium p-toluenesulfonate (0.308 mmol/L) as additive.

Fig. 3 also depicts the dependence of the anodic-peak-current (measured in the ionic-liquid/SPTS solution) on [C_6mim][PTS] concentration for the CMC determination. Again, the CMC is evident from the slope change. Post-micellar behaviors vary across tested solutions (Fig. S3, Supplementary Information), influenced by multiple factors. For electrochemically reversible reactions, peak current is predominantly governed by the concentration of electroactive species and their diffusion coefficient [28]. In contrast, for irreversible or quasireversible reactions, kinetic parameters, such as the charge-transfer coefficient (α) and standard reaction rate constant (k^0) also play crucial roles [28]. Non-faradaic currents further affect the peak current determinations.

The Voltammograms in Fig. S4, Supplementary Information show characteristics of non-reversible reactions. Thus, a lower post-micellar slope suggests that micellar aggregates exhibit greater electrochemical stability toward oxidation—i.e., a smaller reaction rate constant—than unaggregated ionic liquid molecules, as observed for solutions containing $(NH_4)_2SO_4$, KBr, SPTS, and TMAC (Fig. S3). In contrast, solutions containing KCl, Na_2SO_4, CTAB, and SDS exhibited a larger post-micellar slope. Studies have revealed that counterion binding strength at the micellar surface and head-group hydration significantly influence the reaction rates of micellar aggregates in imidazolium-based ionic liquids [34]. In the present work, additional complexity arises due to the diverse additive ions present, each with unique hydration numbers and head-group interactions. Based on available information, the anodic peak observed in the acquired voltammograms (Fig. S4) may be adscribed to the oxidation of the imidazolium cation, most probably the C2 position within the imidazolium ring. [35]

Table 1 summarizes the CMC values determined by UV-Vis absorption spectroscopy, ionic conductivity measurements and cyclic voltammetry. Contrary to what is common [36], all tested methods yielded similar values, underscoring their reliability for CMC determinations in the studied system. Moreover, the level of impurities remaining in the ionic liquid sample after the synthesis procedure must have been sufficiently low, so that highly consistent CMC values were able to be gathered with all tested methods.

The average CMC values listed in Table 1 are all lower than 0.449 mmol/L, the reported CMC of [C_6mim][PTS] in aqueous solution without additives [19]. The values are also comparable to the CMC of the longer-alkyl-chain 3-hexadecyl-1-methylimidazolium p-toluenesulfonate ([C16mim][PTS]) in water, which reportedly is 0.23 mmol/L [29]. As anticipated, the presence of additives enhanced micellar stability. Among the tested compounds, however, CTAB and SDS proved to be the most effective stabilizers, based on the calculated η_{CMC} parameter (Table 1). Inorganic salts are known to reduce electrostatic repulsion among polar

J. Mex. Chem. Soc. **2026**, *70(1):e2548*
Regular Issue

ISSN-e 2594-0317

head groups through charge screening [26], thereby promoting micelle formation. In contrast, the addition of surfactant-type molecules has been associated with increased compactness at the micelle interface [26]. For CTAB and SDS, the presence of long alkyl chains likely facilitates their insertion into the micellar palisade layer [27], which may contribute more significantly to micelle stabilization than electrostatic effects alone.

Regarding the voltametric determinations, the selected electrode material enabled a straightforward response with a convenient solvent window in the anodic region. Despite potential non-faradaic interference and other factors influencing voltammogram shape and peak currents, the electrochemical cell configuration used proved suitable for precise CMC determinations. However, due to the simplicity of ionic conductivity measurements, the latter was preferred for assessing the temperature dependence of the ionic-liquid CMC (Thermodynamic analysis section).

Table 1. Critical Micellar Concentration (CMC) determined by Ultraviolet-Visible Absorption (UV-Vis), Ionic Conductivity (IC) and Cyclic Voltammetry (CV) of 1-methyl-3- hexylimidazolium p-toluenesulfonate ([C_6mim][PTS]) in aqueous solution containing additives: CTAB= Hexadecyltrimethylammonium bromide, TMAC= Tetramethylammonium chloride, SDS= Sodium dodecyl sulfate, SPTS= Sodium p-toluenesulfonate. Degree of CMC-reduction attained by the additive (η_{CMC}).

Additive	**[C_6mim][PTS] CMC (mmol/L)**				η_{CMC}
	UV-Vis	**IC**	**CV**	**Average**	
KBr (0.420 mmol/L)	0.180±0.002	0.186±0.003	0.180±0.001	0.182 ±0.001	0.64
KCl (0.670 mmol/L)	0.195±0.003	0.189±0.002	0.186±0.002	0.190 ±0.002	0.39
Na_2SO_4 (0.352 mmol/L)	0.195±0.002	0.201±0.001	0.195±0.001	0.196 ±0.001	0.72
$(NH_4)_2SO_4$ (0.378 mmol/L)	0.213±0.001	0.204±0.003	0.210±0.002	0.208 ±0.001	0.64
CTAB (0.109 mmol/L)	0.225±0.003	0.242±0.002	0.230±0.003	0.232 ±0.002	1.99
TMAC (0.456 mmol/L)	0.230±0.002	0.236±0.003	0.245±0.003	0.237 ±0.002	0.46
SDS (0.138 mmol/L)	0.225±0.002	0.230±0.002	0.230±0.002	0.228 ±0.001	1.60
SPTS (0.308 mmol/L)	0.219±0.001	0.216±0.002	0.213±0.003	0.215 ±0.002	0.76

Surface tension (γ) of the ionic liquid aqueous-solutions with/without additives

Table 2 reports the surface tension values of [C_6mim][PTS] solutions containing the different tested additives. Compared to the additive-free solution (γ [C_6mim][PTS]), the use of inorganic additives resulted in a surface tension reduction of approximately 50–60 %, while organic additives achieved a more modest reduction of 20–30 %. This apparent greater effectiveness of inorganic additives is also somehow reflected in the Π_{CMC} parameter (Table 2), which is commonly cited in the literature. However, when normalizing by the additive concentration (η_γ parameter, Table 2), CTAB and SDS stand out as the most effective additives to reduce the surface-tension of the [C_6mim][PTS] solution. The high surface-active potential related to the

http://dx.doi.org/10.29356/jmcs.v70i1.2548

J. Mex. Chem. Soc. **2026**, *70(1):e2548*
Regular Issue

ISSN-e 2594-0317

strong amphiphilic nature of those compounds is one of the major reasons for such effect. Generally speaking, the observed decrease in surface tension is attributed to the ability of the additives to compress the electrical double layer around ionic liquid head groups and to compact the micellar interface [26], promoting closer packing at the liquid-air interface.

Table 2. Surface tension (γ), effectiveness of the surface tension reduction (ΠCMC), effectiveness of additive to decrease the surface-tension (ηγ) and Diffusion Coefficient (D) of the 1-methyl-3- hexylimidazolium cation in aqueous solution with/without additives: CTAB= Hexadecyltrimethylammonium bromide, TMAC= Tetramethylammonium chloride, SDS= Sodium dodecyl sulfate, SPTS= Sodium p-toluenesulfonate.

[C_6mim][PTS] (mmol/L)	**Additive**	**γ ([C_6mim][PTS]) (mN/m)**	**γ ([C_6mim][PTS] +Additive) (mN/m)**	**Π_{CMC} (mN/m)**	**η_γ (mN/(m* mmol/L))**	**D @ 301K (10^{-5} cm^2/s)**
0.180	KBr (0.420 mmol/L)	29.80±0.01	14.36±0.01	57.74	36.76	33.80 ±0.01
0.189	KCl (0.670 mmol/L)	28.42±0.01	13.59±0.01	58.51	22.13	2.70 ±0.01
0.195	Na_2SO_4 (0.352 mmol/L)	26.21±0.01	11.10±0.01	61	42.93	28.40 ±0.01
0.207	$(NH_4)_2SO_4$ (0.378 mmol/L)	27.63±0.01	12.16±0.01	59.94	40.93	1.09 ±0.01
0.230	CTAB (0.109 mmol/L)	25.76±0.01	20.52±0.01	51.58	48.07	0.21 ±0.01
0.236	TMAC (0.456 mmol/L)	25.12±0.01	20.01±0.01	52.09	11.21	2.22 ±0.01
0.228	SDS (0.138 mmol/L)	24.56±0.01	18.57±0.01	53.53	43.41	0.51 ±0.01
0.213	SPTS (0.308 mmol/L)	24.92±0.01	17.31±0.01	54.79	24.71	0.57 ±0.01

Diffusion coefficient (*D*) of the ionic-liquid in aqueous solution containing additives

Cyclic voltammograms for the [C_6mim][PTS] solution containing SDS, recorded at 12 different scan rates, are shown in Fig. S5, Supplementary Information. As expected for an electrochemically irreversible process, the oxidation peak potential shifts toward more positive values with increasing scan rate.

Fig. 4 presents the anodic peak current (I_{pa}) as a function of the square root of the scan rate ($v^{1/2}$) for all tested [C_6mim][PTS] solutions. The observed linear trends are consistent with irreversible electrochemical behavior. Slight deviations from linearity at the lowest scan rates likely reflect the transition from quasi-reversible to fully irreversible kinetics, as the quasi-reversible regime is characterized by a nonlinear I_{pa} - $v^{1/2}$ relationship [28]. Thus, to improve the estimation of the diffusion coefficient, the first two data points at low scan rates were excluded from the linear fits.

http://dx.doi.org/10.29356/jmcs.v70i1.2548

J. Mex. Chem. Soc. **2026**, *70(1):e2548*
Regular Issue

ISSN-e 2594-0317

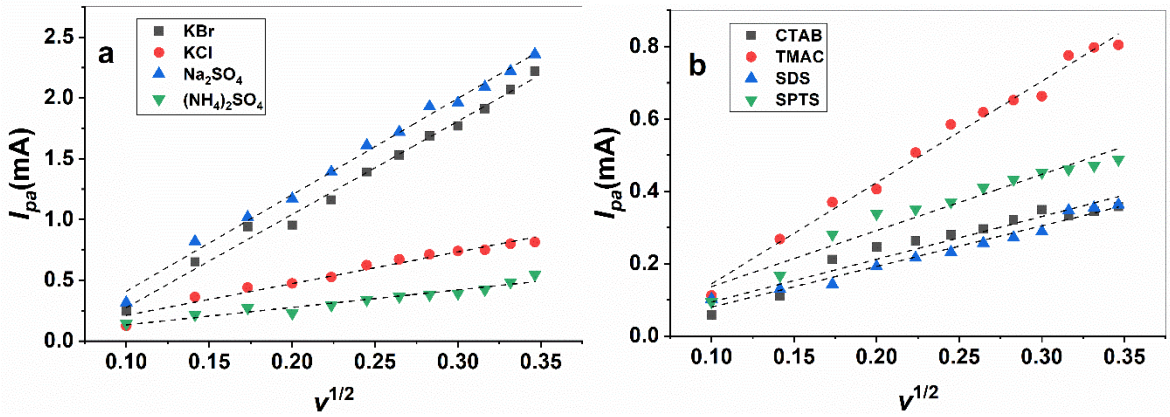

Fig. 4. Anodic peak-current (I_{pa}) vs square root of voltammetric scan-rate (v) of the 1-methyl-3-hexylimidazolium p-toluenesulfonate ([C_6mim][PTS]) aqueous solutions (concentration as in Table 2). **(a)** inorganic additives: KBr (0.420 mmol/L), KCl (0.670 mmol/L), Na_2SO_4 (0.352 mmol/L), $(NH_4)_2SO_4$ (0.378 mmol/L); **(b)** organic additives: CTAB= Hexadecyltrimethylammonium bromide (0.109 mmol/L), TMAC= Tetramethylammonium chloride (0.456 mmol/L), SDS= Sodium dodecyl sulfate (0.138 mmol/L), SPTS= Sodium p-toluenesulfonate (0.308 mmol/L).

The diffusion coefficient of the [C_6mim] cation, calculated using Equations 3 and 4, is presented in the last column of Table 2. The lowest value obtained closely matches that previously reported for [C_6mim][PTS] in aqueous solution (0.228×10^{-5} cm^2/s, at room temperature) based on voltammetric measurements using a rotating disk electrode [16]. To the best of our knowledge, no additional reports on the diffusion coefficient of [C_6mim][PTS] are available in the literature. Nevertheless, further comparisons can be made with structurally related systems. For instance, the self-diffusion coefficient of [C_6mim][$(CF_3SO_2)_2N$] cation is approximately 2×10^{-7} cm^2/s at 301 K [37]. On the other side, in aqueous medium and at high dilution, [C_4mim][$(CF_3SO_2)_2N$] and [C_4mim][$OcSO_4$] are reported to have diffusion coefficients around 1.1×10^{-5} cm^2/s at 303.1 K [38]. Given that [C_6mim] is only two methylene units longer than [C_4mim], and that the [PTS] anion appears not much bulkier than [NTf_2] or [$OcSO_4$], the diffusion coefficients reported here seem consistent with expectations.

As previously discussed, non-faradaic currents can significantly affect peak current measurements in voltammetry. Because these capacitive contributions could not be entirely removed from the recorded voltammograms, part of the variation observed in the calculated diffusion coefficients may be attributed to differences in the structure of the electrical double layer adjacent to the electrode surface. Notably, higher diffusion coefficients were obtained for solutions containing inorganic additives, which had a greater ionic strength than the organic salt solutions. Increased ionic strength results in a more compressed electrical double layer, leading to higher capacitance and larger non-faradaic currents. Baseline correction can be applied to well behaved voltammograms in order to minimize the contribution of non-faradaic currents. This approach enhances the accuracy of peak current determinations [28]. Furthermore, the magnitude of non-faradaic currents can be considerably reduced by employing electrodes with markedly smaller surface areas, such as microelectrodes or ultramicroelectrodes [28].

Thermodynamic analysis

The temperature dependence of the critical micellar concentration (CMC) for [C_6mim][PTS] in aqueous solution is presented in Fig. 5. Across all tested systems, the CMC increases nearly linearly with temperature over the range 300.15 - 318.15 K. This trend is consistent with the general understanding that micelle formation becomes less favorable at elevated temperatures due to increased thermal motion, which disrupts the ordered micellar structures [39].

http://dx.doi.org/10.29356/jmcs.v70i1.2548

J. Mex. Chem. Soc. **2026**, *70(1):e2548*
Regular Issue

ISSN-e 2594-0317

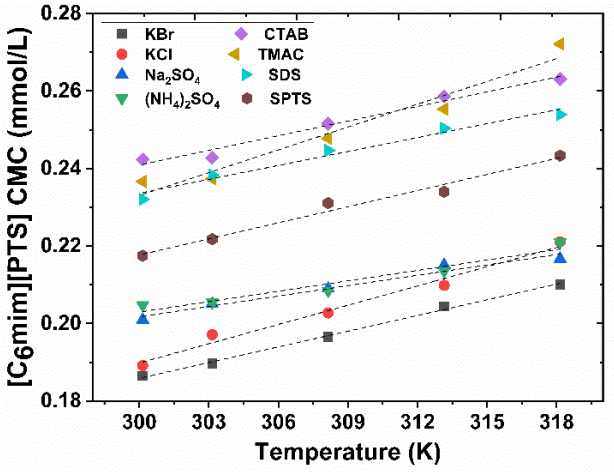

Fig. 5. Critical micellar concentration (CMC) of the 1-methyl-3- hexylimidazolium p-toluenesulfonate ([C_6mim][PTS]) aqueous solution (concentration as in Table 2) containing additives: KBr (0.420 mmol/L), KCl (0.670 mmol/L), Na_2SO_4 (0.352 mmol/L), $(NH_4)_2SO_4$ (0.378 mmol/L), CTAB= Hexadecyltrimethylammonium bromide (0.109 mmol/L), TMAC= Tetramethylammonium chloride (0.456 mmol/L), SDS= Sodium dodecyl sulfate (0.138 mmol/L), SPTS= Sodium p-toluenesulfonate (0.308 mmol/L).

Tables S1 - S8 in the Supplementary Information provide the raw conductivity data used to determine the CMC values, while Figures S6–S13, Supplementary Information show the corresponding conductivity plots. The β parameter, representing the degree of counterion binding to the micelle, was also extracted from these plots and is shown in Fig. 6(a). Notably, β remains relatively constant with temperature for each additive, suggesting that the extent of counterion association is not strongly temperature-dependent within the studied range. A comparison of β values reveals that Na_2SO_4 and $(NH_4)_2SO_4$ exhibit the highest β values of the inorganic-additives group. This behavior is likely due to the high charge density and kosmotropic nature of the SO_4^{2-} anions, which enhance electrostatic interactions at the micellar interface. In contrast, organic additives such as CTAB and SPTS, despite their surfactant-like structures, show lower β values possibly due to steric hindrance or competitive interactions at the micelle surface.

Fig. 6(b) – 6(d) present the temperature dependence of the micellization Gibbs free energy (ΔG_m), enthalpy (ΔH_m), and entropy (ΔS_m), respectively (corresponding numerical data are provided in Table S9). For the ΔH_m determinations, all systems exhibited a markedly $ln\left(\frac{CMC}{55.4}\right)$ vs. T linear trend, so the data were fitted to a straight line whose slope corresponds to the required derivative in Eq. 6.

Across all systems, ΔG_m is negative, confirming that micellization is spontaneous under the studied conditions. Interestingly, ΔG_m becomes slightly more negative as temperature increases, a trend attributed to the relative stability of the β-parameter with respect to temperature. Similar to ΔG_m, the micellization enthalpy (ΔH_m) is negative throughout the entire temperature range, indicating that micellization is an exothermic process. However, the magnitude of ΔH_m varies in general with the nature of the additive. In solutions containing CTAB and SDS, ΔH_m values are comparatively lower in magnitude, suggesting that micellization in these systems relies more on hydrophobic interactions and structural compatibility than on electrostatic stabilization. In contrast, more exothermic ΔH_m values are observed in the presence of inorganic salts such as KBr and KCl, consistent with enhanced charge screening. TMAC presents an interesting case: although it is an organic additive, its compact, symmetric structure and full dissociation in water allow it to behave more closely to inorganic salts in this context.

The entropy of micellization (ΔS_m) is positive in all cases, reflecting the increased disorder associated with the release of structured water molecules from the hydration shells of the surfactant ions and the formation of dynamic micellar aggregates. Relatively large ΔS_m values are observed for CTAB and SDS, consistent with entropy-driven micellization dominated by hydrophobic interactions from long-chain

J. Mex. Chem. Soc. **2026**, *70(1):e2548*
Regular Issue

ISSN-e 2594-0317

amphiphiles. However, ΔS_m decreases slightly with increasing temperature, while ΔH_m becomes more negative. This shift suggests that at higher temperatures, micellization may become increasingly enthalpy-driven, a classic example of enthalpy-entropy compensation, a well-documented phenomenon in surfactant systems [39]. It underscores the delicate balance of forces, i.e. electrostatic, hydrophobic, and entropic, that govern self-assembly in ionic liquid solutions.

When comparing additives, a clear thermodynamic distinction emerges. Inorganic salts promote micellization primarily through enthalpic contributions, driven by charge screening and enhanced counterion binding. In contrast, organic additives, particularly CTAB and SDS, favor micellization through entropic gains associated with hydrophobic interactions and micelle compaction. This distinction aligns with the structural roles discussed earlier (Section 3.1): inorganic ions modulate the electrostatic environment, while amphiphilic organics integrate into the micellar interface, altering its internal organization and dynamics. Despite these differences, the overall thermodynamic profiles of the systems remain qualitatively similar: micellization is spontaneous, exothermic, and entropically favored across all conditions. This robustness suggests that [C₆mim][PTS] is a versatile surface-active ionic liquid whose aggregation behavior can be finely tuned through additive selection without compromising its fundamental self-assembly characteristics.

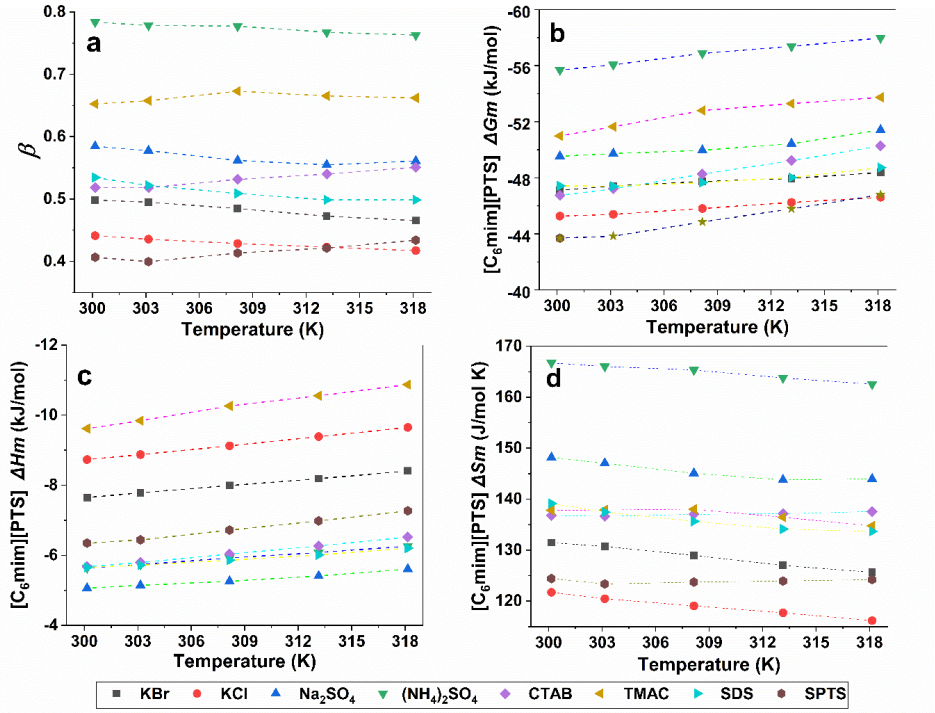

Fig. 6. Thermodynamics parameters of the 1-methyl-3-hexylimidazolium p-toluenesulfonate ([C_6mim][PTS]) aqueous solutions (concentration as in Table 2). a) β-parameter; b) micellization Gibbs energy (ΔG_m); c) micellization enthalpy (ΔH_m); micellization entropy (ΔS_m). Additives: KBr (0.420 mmol/L), KCl (0.670 mmol/L), Na_2SO_4 (0.352 mmol/L), $(NH_4)_2SO_4$ (0.378 mmol/L), CTAB= Hexadecyltrimethylammonium bromide (0.109 mmol/L), TMAC= Tetramethylammonium chloride (0.456 mmol/L), SDS= Sodium dodecyl sulfate (0.138 mmol/L), SPTS= Sodium p-toluenesulfonate (0.308 mmol/L).

Conclusions

The present study demonstrates that the micellization behavior and interfacial properties of the short-alkyl-chain surface-active ionic liquid [C₆mim][PTS] can be effectively modulated through the addition of

J. Mex. Chem. Soc. **2026**, *70(1):e2548*
Regular Issue

ISSN-e 2594-0317

common organic and inorganic additives. All tested additives reduced the critical micellar concentration (CMC) and surface tension of the ionic liquid in aqueous solution, with the most pronounced effects observed for amphiphilic organic additives such as CTAB and SDS. These compounds, due to their structural similarity and long hydrophobic chains, integrate into the micellar interface and significantly enhance micelle stability, achieving CMC values comparable to those of longer-chain imidazolium-based ionic liquids.

Thermodynamic analysis revealed that micellization remains spontaneous, exothermic, and entropically favored across the studied temperature range (300.15–318.15 K). Inorganic salts promoted micellization primarily through enthalpic contributions, driven by charge screening and enhanced counterion binding, while organic additives favored entropy-driven micellization via hydrophobic interactions and micelle compaction. TMAC, although organic, exhibited behavior more akin to inorganic salts due to its compact, fully dissociated structure.

Although diffusion coefficients derived from electrochemical measurements are influenced by non-faradaic current effects, they provide a valuable preliminary estimate and serve as a useful reference point for more precise determinations in future studies.

Importantly, all three experimental techniques, UV-Vis spectroscopy, ionic conductivity, and cyclic voltammetry, proved reliable for CMC determination. Cyclic voltammetry, in particular, offered the added advantage of enabling diffusion coefficient estimates, making it a valuable tool for comprehensive micellization studies.

Overall, [C_6mim][PTS] emerges as a versatile and tunable surface-active ionic liquid, with aggregation properties that can be finely adjusted through additive selection. These findings not only expand the fundamental understanding of short-chain surface-active ionic-liquids of neutral character but also support their potential application in environmentally relevant processes such as oil-water emulsion treatment and surfactant-assisted separations.

Acknowledgements

E.E.V.N gratefully acknowledges the generous postdoctoral-research-scholarship provided by the "Programa de Becas Posdoctorales" of the "Dirección General de Asuntos del Personal Académico –DGAPA- de la Universidad Nacional Autónoma de México - UNAM", and the productive collaboration with R. Mayén-Mondragón. Financial support from the "Facultad de Química de la Universidad Nacional Autónoma de México" through project PAIP 5000-9150 is as well gratefully acknowledged.

References

1. Zaitsau, D. H.; Kabo, G. J.; Strechan, A. A.; Paulechka, Y. U.; Tschersich, A.; Verevkin, S. P.; Heintz, A. *J. Phys. Chem. A.* **2006**, *110*, 7303–7306. DOI: https://pubs.acs.org/doi/10.1021/jp060896f
2. Tröger-Müller, S.; Antonietti, M.; Liedel, C. *Phys. Chem. Chem. Phys.* **2018**, *20*, 11437–11443. DOI: https://doi.org/10.1039/C8CP00311D
3. Talip, R. A. A.; Yahya, W. Z. N.; Bustam, M. A. *E3S Web Conf.* **2021**, *287*, 02015. DOI: https://doi.org/10.1051/e3sconf/202128702015
4. Yang, H.; Liu, Y.; Ning, H.; Lei, J.; Hu, G. *RSC Adv.* **2017**, *7*, 33231–33240. DOI: https://doi.org/10.1039/c7ra05601j
5. Kaur, G.; Kumar, H.; Singla, M. *J. Mol. Liq.* **2022**, *351*, 118556. DOI: https://doi.org/10.1016/j.molliq.2022.118556
6. Buettner, C. S.; Cognigni, A.; Schröder, C.; Bica-Schröder, K. *J. Mol. Liq.* **2022**, *347*, 118160. DOI: https://doi.org/10.1016/j.molliq.2021.118160
7. Goutham, R.; Rohit, P.; Vigneshwar, S. S.; Swetha, A.; Arun, J.; Gopinath, K. P.; Pugazhendhi, A. *J. Mol. Liq.* **2022**, *349*, 118150. DOI: https://doi.org/10.1016/j.molliq.2021.118150

J. Mex. Chem. Soc. **2026**, *70(1):e2548*
Regular Issue

ISSN-e 2594-0317

8. Zhang, L.; Yu, R.; Zhou, M.; Wang, C.; Zhang, D.; Ren, W.; Shao, Y. *Food Chem.* **2022**, *379*, 132161. DOI: https://doi.org/10.1016/j.foodchem.2022.132161
9. Kaur, R.; Kumar, H.; Singla, M. *J. Mol. Liq.* **2022**, *354*, 118904. DOI: https://doi.org/10.1016/j.molliq.2022.118904
10. McNeice, P.; Marr, P. C.; Marr, A. C. *Catal. Sci. Technol.* **2021**, *11*, 726–741. DOI: https://doi.org/10.1039/d0cy02274h
11. Earle, M. J.; Seddon, K. R. *Pure Appl. Chem.* **2000**, *72*, 1391–1398.
12. Kumar, R.; Sharma, A.; Sharma, N.; Kumar, V.; Sinha, A. K. *Eur. J. Org. Chem.* **2008**, *33*, 5577–5582. DOI: https://doi.org/10.1002/ejoc.200800657
13. Potdar, M. K.; Rasalkar, M. S.; Mohile, S. S.; Salunkhe, M. M. *J. Mol. Catal. A Chem.* **2005**, *235*, 249–252. DOI: https://doi.org/10.1016/j.molcata.2005.04.007
14. Xia, M.; Lu, Y. D. *J. Mol. Catal. A Chem.* **2007**, *265*, 205–208. DOI: https://doi.org/10.1016/j.molcata.2006.10.004
15. Biedroń, T.; Kubisa, P. *J. Polym. Sci. A Polym. Chem.* **2004**, *42*, 3230–3235. DOI: https://doi.org/10.1002/pola.20158
16. Lara Hernández, A. R.; Gallardo Rivas, N. V.; Páramo García, U.; Mayén-Mondragón, R.; Brachetti Sibaja, S. B. *Int. J. Electrochem. Sci.* **2021**, *16*, 21101. DOI: https://doi.org/10.20964/2021.10.49
17. Amde, M.; Liu, J. F.; Pang, L. *Environ. Sci. Technol.* **2015**, *49*, 12611–12627. DOI: https://pubs.acs.org/doi/10.1021/acs.est.5b03123
18. Wei, Y.; Wang, F.; Zhang, Z.; Ren, C.; Lin, Y. *J. Chem. Eng. Data.* **2014**, *59*, 1120–1129. DOI: https://doi.org/10.1021/je400861g
19. Villalobos Neri, E. E.; Páramo García, U.; Mayen-Mondragon, R.; Gallardo-Rivas, N. V. *Int. J. Electrochem. Sci.* **2021**, *16*, 210611. DOI: https://doi.org/10.20964/2021.06.59
20. Del Ángel Gómez, E. J.; Gallardo Rivas, N. V.; Paramo García, U.; Díaz Zavala, N. P.; Banda Cruz, E. E.; Martínez Orozco, R. D.; García-Alamilla, R. *Petrol. Sci. Technol.* **2022**, *40*, 2163–2178. DOI: https://doi.org/10.1080/10916466.2022.2036760
21. El Shafiee, C. C.; El-Nagar, R. A.; Nessim, M. I.; Khalil, M. M. H.; Shaban, M. E.; Alharthy, R. D.; Ismail, D. A.; Abdallah, R. I.; Moustafa, Y. M. *Arab. J. Chem.* **2021**, *14*, 103123. DOI: https://doi.org/10.1016/j.arabjc.2021.103123
22. McFarlane, J.; Ridenour, W. B.; Luo, H.; Hunt, R. D.; DePaoli, D. W.; Ren, R. X. *Sep. Sci. Technol.* **2005**, *40*, 1245–1265. DOI: https://doi.org/10.1081/SS-200052807
23. Nazar, M.; Ahmad, A.; Hussain, S. M. S.; Moniruzzaman, M. *Mar. Pollut. Bull.* **2024**, *202*, 116311. DOI: https://doi.org/10.1016/j.marpolbul.2024.116311
24. Rather, M. A.; Rather, G. M.; Pandit, S. A.; Bhat, S. A.; Bhat, M. A. *Talanta.* **2015**, *131*, 55–58. DOI: https://doi.org/10.1016/j.talanta.2014.07.046
25. Zha, J. P.; Zhu, M. T.; Qin, L.; Wang, X. H. *Spectrochim. Acta A Mol. Biomol. Spectrosc.* **2018**, *196*, 178–184. DOI: https://doi.org/10.1016/j.saa.2018.02.015
26. Tariq, M.; Freire, M. G.; Saramago, B.; Coutinho, J. A. P.; Lopes, J. N. C.; Rebelo, L. P. N. *Chem. Soc. Rev.* **2012**, *41*, 829–868. DOI: https://doi.org/10.1039/C1CS15146K
27. Fu, D.; Gao, X.; Huang, B.; Wang, J.; Sun, Y.; Zhang, W.; Kan, K.; Zhang, X.; Xie, Y.; Sui, X. *RSC Adv.* **2019**, *9*, 28799–28807. DOI: https://doi.org/10.1039/C9RA04226A
28. Bard, A. J.; Faulkner, L. R., in: *Electrochemical Methods: Fundamentals and Applications*; 2nd ed.; John Wiley & Sons: New York, 2001.
29. Singh, G.; Singh, G.; Kang, T. S. *J. Phys. Chem. B.* **2016**, *120*, 1092–1105. DOI: https://doi.org/10.1021/acs.jpcb.5b09688
30. Oremusová, J.; Vitková, Z.; Vitko, A.; Tárník, M.; Miklovičová, E.; Ivánková, O.; Murgaš, J.; Krchňák, D. *Molecules.* **2019**, *24*, 651. DOI: https://doi.org/10.3390/molecules24030651
31. Medoš, Ž.; Bešter-Rogač, M. *J. Chem. Thermodyn.* **2015**, *83*, 117–122. DOI: https://doi.org/10.1016/j.jct.2014.12.011

J. Mex. Chem. Soc. **2026**, *70(1):e2548*
Regular Issue

ISSN-e 2594-0317

32. More, U. U.; Vaid, Z. S.; Rajput, S. M.; Malek, N. I.; El Seoud, O. A. *Colloid Polym. Sci.* **2017**, *295*, 2351–2361. DOI: https://doi.org/10.1007/s00396-017-4210-x
33. Sao, S.; Mukherjee, I.; De, P.; Chaudhuri, D. *Chem. Commun.* **2017**, *53*, 3994–3997. DOI: https://doi.org/10.1039/C7CC00554G
34. Friesen, S.; Buchecker, T.; Cognigni, A.; Bica, K.; Buchner, R. *Langmuir.* **2017**, *33*, 9844–9856. DOI: https://doi.org/10.1021/acs.langmuir.7b02201
35. De Vos, N.; Maton, C.; Stevens, C. V. *ChemElectroChem.* **2014**, *1*, 1258–1270. DOI: https://doi.org/10.1002/celc.201402086
36. Racaud, C.; Groenen Serrano, K.; Savall, A. *J. Appl. Electrochem.* **2010**, *40*, 1845–1851. DOI: https://doi.org/10.1007/S10800-010-0145-3
37. Tokuda, H.; Hayamizu, K.; Ishii, K.; Susan, M. A. B. H.; Watanabe, M. *J. Phys. Chem. B.* **2005**, *109*, 6103–6110. DOI: https://doi.org/10.1021/jp044626d
38. Heintz, A.; Lehmann, J. K.; Schmidt, E.; Wandschneider, A. *J. Solution Chem.* **2009**, *38*, 1079–1083. DOI: https://doi.org/10.1007/s10953-009-9431-2
39. Chauhan, S.; Sharma, K. *J. Chem. Thermodyn.* **2014**, *71*, 205–211. DOI: https://doi.org/10.1016/j.jct.2013.12.019